Chapter 6

Mixed adsorption of TTF and TCNQ on Au(111)

In this chapter the adsorption and supramolecular assembly of TTF and TCNQ on Au(111) is discussed as well as the electronic properties developed in the donor-acceptor system. Metal/organic interfaces are a subject of increasing interest in the condensed matter community. Organic materials have many advantageous properties that are, among others, ease of growth, low cost, and tailoring by chemical synthesis. However, they posses narrow bands and low electron mobility, which makes them not so efficient for their use in electronic devices. The combination of molecular layers with an inorganic crystal opens a new perspective for increasing the efficiency of the organic device. The high carrier mobility of the crystal may develop, together with the above described properties of the organic materials, interesting combined phenomenology at the organic/inorganic interface.

Here we report on how the electronic properties of an Au(111) surface can be modified upon adsorption of a TTF-TCNQ layer. A combination of local STS measurements and DFT calculations show the development of dispersive hybrid bands with both molecular and metallic surface state character at the organic/inorganic interface. Such bands are spatially localized due to the symmetry of the TTF-TCNQ adlayer and present a reduced dimensionality in their dispersion.

6.1 Structural properties of an ultra-thin film of TTF-TCNQ on Au(111)

The individual adsorption of TTF and TCNQ at room temperature produces significantly different ordered structures (Chapter 5). On the one hand, TTF forms a molecular Wigner crystal upon charge transfer with the surface that results in the formation of a surface patterned lattice based on long-range repulsive interactions of electrostatic nature. On the other hand, TCNQ self-assembles in highly ordered islands in the frame of a hydrogen-bond network formed upon stabilization via C$\equiv$N$\cdots$H-C bonds.

In spite of these homomolecular stable structures, TTF and TCNQ form spontaneously mixed domains when co-deposited on the Au(111) metal. Nevertheless, the growth of the heteromolecular system needs to be thermally activated. The minimum

required temperature at which TTF and TCNQ recognize and self-assemble is 150 K - 200 K.

Different mixed structures are obtained depending on the concentration of each molecular entity on the surface. Fig. 6.1 shows two islands with the different domains that can be found. An excess of TTF reveals the formation of a mixed phase with stoichiometry 2(TTF): 1(TCNQ), as shown in Fig. 6.1(a). This structure do not have any corresponding bulk arrangement. Upon co-deposition with excess of TCNQ molecules, TTF and TCNQ form one-dimensional homomolecular chains, giving rise to a highly anisotropic molecular structure that follows the symmetry directions of the underlying Au(111) surface (Fig. 6.1(b)). The unit cell of this structure contains one TTF and one TCNQ molecule (1:1 stoichiometry). All the TTF available assembles with the TCNQ, and the surplus of TCNQ remains in homomolecular regions.

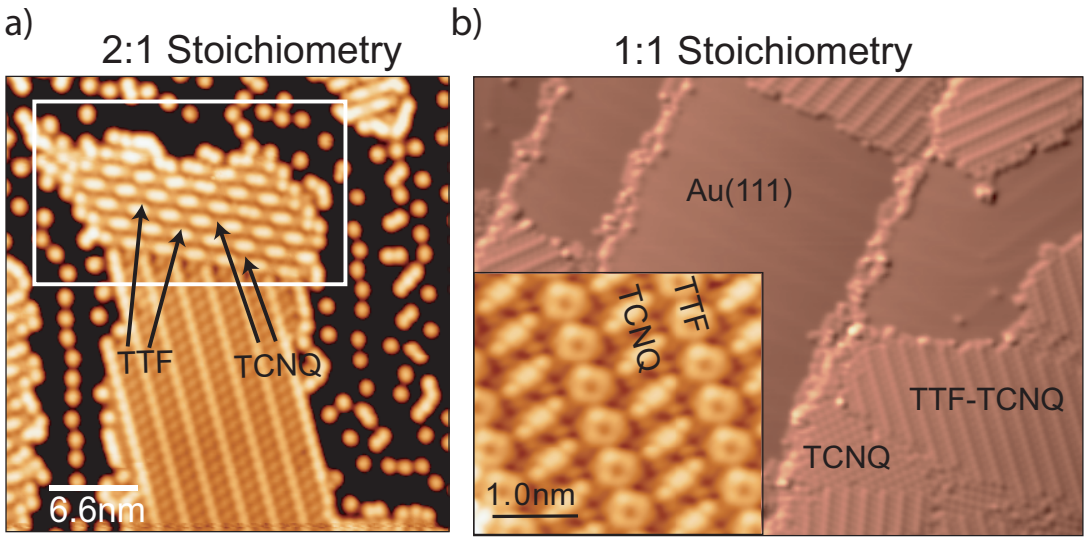

Figure 6.1: (a) STM image of a domain with both 1:1 and 2:1 (inside the rectangle) stoichiometries (V = 1.2 V, I = 0.1 nA). Bright protrusions are TTF molecules and low correspond to TCNQ. Surplus of TTF adsorbs following the repulsive behavior described in Chapter 5. (b) STM image of a large self-assembled domain obtained with surplus of TCNQ (V = 1.9 V, I = 0.1 nA). The 1:1 mixed phase areas follow different orientations according to the symmetry directions of the underlying surface. The inset (V = 0.3 V, I = 0.4 nA) shows a 1:1 mixed domain with intramolecular resolution.

The homomolecular row structure of the 1:1 TTF-TCNQ phase resembles the anisotropic bulk structure, which has been presented in the introduction of Part II. However, while in bulk the molecules within the row stabilize by π-π interactions, TTF and TCNQ are adsorbed almost planar on Au(111). This can be inferred from the STM images with intra-molecular resolution (inset of Fig. 6.1(b)). The imaged TTF isosurfaces are similar to the isolated case (section 5.1), reflecting a slight tilt of two S atoms. TCNQ changes slightly its orbital shape with respect to the pure island

case: when embedded in a mixed TTF-TCNQ domain, the orbital fingerprint at the CN ending groups weakens.

The interaction of the π electrons with the metal surface is stronger than intermolecular π-stacking forces. In consequence, TTF and TCNQ do not aggregate in the first stages of growth in the bulk-like stacking. From the STM images we can tentatively construct a model of the planar self-assembled TTF-TCNQ phase (Fig. 6.2) where the molecules interact and form a hydrogen bond network by short range C≡N$\cdots$H-C connections.

The resemblance of the structure of this phase with the bulk organization suggests that the one-dimensional arrangement in rows can also be induced by donor-acceptor interactions. Among others, we will address this question in the following sections of this chapter.

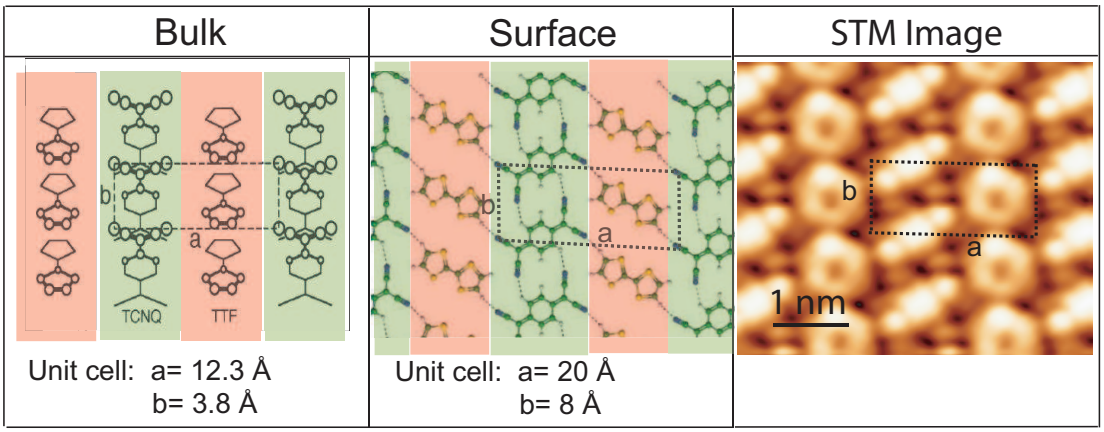

Figure 6.2: Comparison between the molecular unit cell of bulk (left) built up via π stacking of the molecular components and the surface unit cell (center), where the molecular structure is stabilized via hydrogen bonds. As a consequence of the planar adsorption of TTF and TCNQ on Au(111), the surface unit cell is slightly larger than in the bulk case. An STM image (right) of the mixed domain is presented to illustrate the surface unit cell.

6.2 Electronic properties of a hybrid metal-organic interface

Fig. 6.3(c) presents an STM image of a boundary between a pure TCNQ island and a mixed TTF-TCNQ domain. The conductance (dI/dV) spectra of TCNQ embedded in a pure island and located on the mixed phase are compared in Fig. 6.3(a) and (b). Pure TCNQ islands show the resonance related to the LUMO at 0.7 eV and the shifting of the Au(111) surface state. These two fingerprints are modified on the mixed TTF-TCNQ phase. Instead of the broad LUMO peak, a sharp resonance arises at 0.3 eV (IS1 in Fig. 6.3(b)) located on the TCNQ rows. On the TTF a similar but

broader spectral fingerprint appears at 0.8 eV (IS2). In addition to the appearance of these new resonances, the distinctive onset of the surface state is not observed on the mixed TTF-TCNQ layer. A mapping of the dI/dV spectra taken along the main directions of the layer (Fig. 6.3(d) and (e)) provides a more complete picture of the spatial location of resonances IS1 and IS2. The line scans taken along Y (crossing TTF and TCNQ rows) reveal a localization of the resonances within the molecular chains: IS1 has a stronger signal on the TCNQ rows, while IS2 is mainly localized on the TTF rows. Furthermore, the IS1 resonance is much thinner than IS2, with a FWHM of the first being half the value of the second. An extra resonance appears on the TTF molecules at 1.7 eV which is related to the LUMO of the molecule, as reported by DFT calculations of TTF/Au(111) (section 5.1.2). Line scans taken along a TCNQ row (direction X) and finishing on the pure TCNQ domain, show a strong localization of the IS1 resonance within the rows and does not present an intensity dependence on the lateral position of the STM tip (on top or between molecules). The resonance IS1 vanishes at the end of the mixed domain. At the zone boundary, both the pure TCNQ LUMO and the shifted surface state appear and increase their intensity when the STM tip leaves the border and gets onto the TCNQ island.

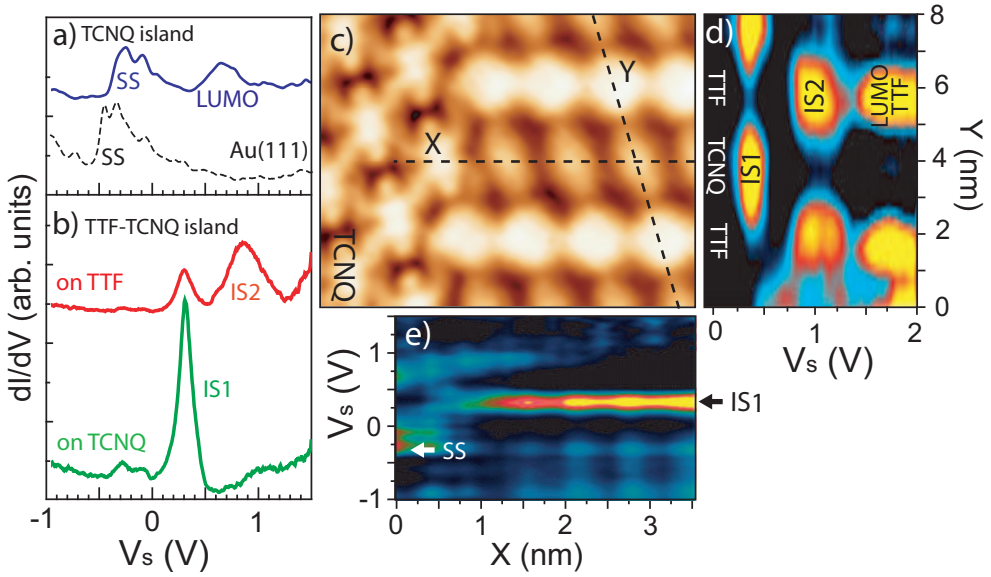

Figure 6.3: Comparison of dI/dV spectra of (a) TCNQ pure islands (spectrum taken on a clean Au(111) region shown for comparison) and (b) TTF and TCNQ in mixed TTF-TCNQ islands (V = 1.9 V, I = 1 nA, V_{ac} = 3.5 V_{rms}). (d,e) The differential conductance spectra are mapped along the dashed lines shown in the STM image (c) (V = 1.9 V, I = 0.07 nA). The maps clearly show the spatial localization of IS1 and IS2 features on TCNQ and TTF rows, respectively.

The origin of these peaks can not be associated to resonant tunneling through molecular states, since the TTF LUMO is located at 1.7 eV. Furthermore, they can not be understood in a simple scenario of molecular level alignment since the resonances IS1 and IS2 are not only a shift but also involve an important change in linewidth.

STM measurements also reveal a difference in the orbital shape of TCNQ depending on whether it is embedded in a pure TCNQ island or located in a TTF-TCNQ mixed domain. Isolated TCNQ or TCNQ nucleated in islands present the characteristic orbital shape which resembles the LUMO for bias voltages above 0.7 eV. On TTF-TCNQ islands, its structure on CN terminations appears weaker.

In order to rule out a possible molecular degradation upon chemical reaction between TTF and TCNQ during the formation of the mixed layer, lateral manipulation (LM) of the molecules has been performed, as sketched in Fig. 6.4.

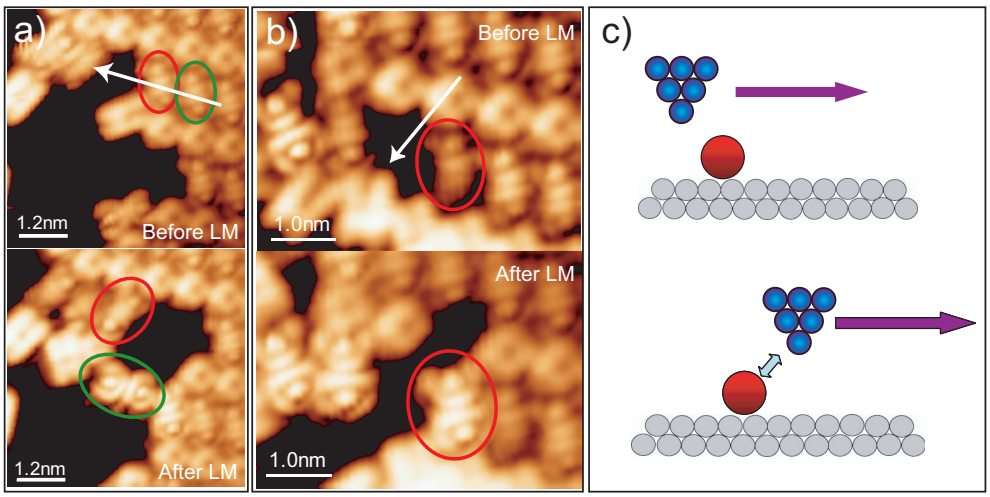

Figure 6.4: (a) and (b) show lateral manipulation with the STM tip of TCNQ molecules. being taken from the mixed TTF-TCNQ phase. The white arrow indicates the movement of the tip during the manipulation. As soon as TCNQ is out of the mixed TTF-TCNQ self-assembled phase, the LDOS recovers its LUMO shape, with signal at the cyano groups. The resistance of the tunneling junction during LM is 2 MΩ (V = 0.1 V, I = 50 nA). (c) Lateral Manipulation scheme. The tip is driven closer to the surface and, by means of electrostatic interactions with the adsorbate, provokes its motion on the surface.

By means of LM we can separate the TCNQ from the mixed phase, which recovers then its distinctive LUMO shape. We can confirm that TCNQ molecules remain intact upon co-adsorption with the TTF on the Au(111) surface. Thus, the spectral features IS1 and IS2 must be a new fingerprint of a novel interaction between the anisotropic molecular adlayer and the Au(111) surface.

A hint about the origin of these peaks is the dispersive behaviour of IS1. dI/dV maps taken at energies above this resonance display an oscillatory pattern (Fig. 6.5(a)-(f)) with a periodicity larger than the molecular corrugation and dependent on the sample bias voltage. Such behavior is characteristic of a quantum interference system. These oscillations are present only on the TCNQ rows. Therefore, they can be considered as a fingerprint of a quasi one-dimensional electron band, similar to the case of a particle in a box. Borders of the islands and defects act as scattering centers. The phase of the electrons wavefunctions is set at those points and, in consequence, forming

the constructive/destructive interference patterns. In analogy to the basic quantum mechanic problem of a particle in a one-dimensional box, for the oscillations to appear the energy has to fulfill the equation $E_n = \hbar^2\pi^2n^2/(2mL^2)$, where m is the mass of the particle, L is the length of the box and n is an integer number. According to this equation, we might observe the interference pattern for a certain energy only for those rows with the appropriate length, as presented by the arrows in Fig. 6.5(a)-(f).

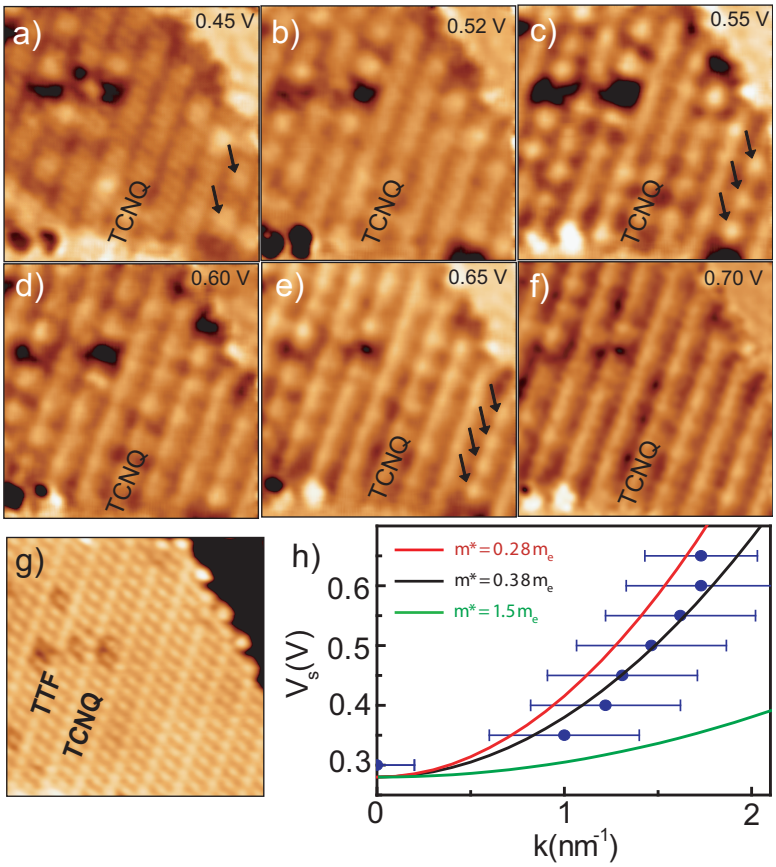

Figure 6.5: (a-f) dI/dV maps (I = 1 nA, V_{ac} = 25 V_{rms}) of a TTF-TCNQ island (STM image presented in (g)) at sample bias above the onset of the IS1 resonance (I = 1.0 nA, 16x16 nm^2). The arrows mark the maxima position of the oscillatory pattern when the boundary conditions fulfill the creation of maxima along the molecular chains. (h) Dispersion obtained upon FFT analysis of the modulation. The black line is the fit to the data. Red and green curves are presented for comparison with dispersion obtained in a metal surface state and a metalorganic compound, respectively.

The change in wavelength is fitted to a parabolic dispersion relation $E(k) = E_0 + \hbar^2k^2/2m^*$, where E_0 is the binding energy of the parabolic band and m* is the effective mass of the particles in free motion [164]. The fitting results in an effective mass of value $m^* = (0.38 \pm 0.05)m_e$ as presented in Fig. 6.5(h). As pointed out in the figure, such dispersion is of quasi-metallic character. Its effective mass is closer to the characteristic value of electrons embedded in the surface state ($0.28m_e$ for a Au(111)

surface) [138, 163] than to the dispersion expected for a pure molecular conductor (above $1m_e$) [100]. Therefore, the feature IS1 is presumably related to the underlying metal states [165, 166].

Then, the appearance of two resonances with different lineshape observed at different regions of the self-assembled domain, and the dispersive behavior of electrons along the TCNQ rows indicates that the system can not be simply treated as a molecular layer adsorbed weakly on the surface. Instead, these results point towards the creation of a new system consisting of molecular orbitals anisotropically hybridized with metal states located at the interface.

6.2.1 DFT modeling of the TTF-TCNQ/Au(111) interface

Theoretical calculations will help to decipher the role of the molecular and metal component at the interface. The DFT calculations presented in this section are carried out in the framework of a collaboration with Prof. Andrés Arnau and Nora González-Lakunza at DIPC, San Sebastián (Spain) and Prof. Nicolás Lorente at CIN2-CSIC, Barcelona (Spain).

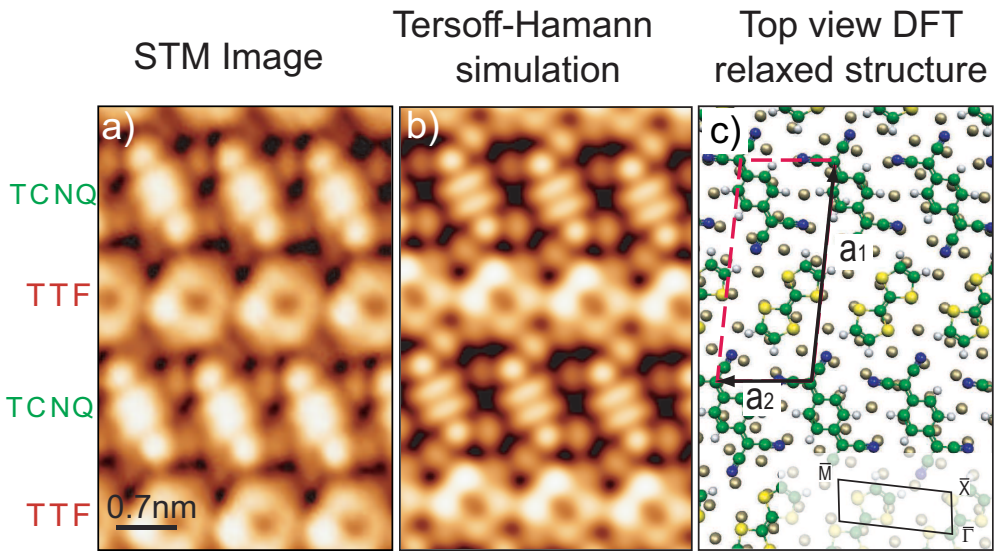

Figure 6.6: (a) Intramolecular structure of TTF and TCNQ resembling the shape of the HOMO and the LUMO, respectively (I = 0.4 nA, V = 0.3 V). Simulated constant current STM image at V = 1.0 V, using the Tersoff-Hamann approach on the DFT relaxed structure shown in (c). The unit cell vectors in real space, a_1 and a_2, are superimposed in (c). The inset in (c) shows the surface Brillouin zone obtained from the reciprocal vectors b_1 and b_2.

The unit cell chosen for the calculations is represented in Fig. 6.6(c). It is designed after the experimental data (Fig. 6.6(a), corroborated by the simulated STM image, Fig. 6.6(b)) and follows the symmetry of the molecular adlayer. The Au(111) surface is simulated by a slab of four layers of gold, with the last one passivated with H in

order to obtain a good fingerprint of the Au(111) surface state. The inset in Fig. 6.6(c) shows the surface Brillouin zone (SBZ) that is defined by the points $\overline{\Gamma}$ = (0,0), $\overline{X}$ = (1/2,0) and $\overline{M}$ = (1/2,1/2), in units of the reciprocal vectors b_1 and b_2. The symmetry directions $\overline{\Gamma X}$ and $\overline{XM}$ correspond to the directions across and along the molecular rows, respectively.

Role of molecular orbitals at the TTF-TCNQ/Au(111) interface

The computation of the PDOS and the induced electron density of the relaxed TTF-TCNQ layer on Au(111) provides information about both the interaction with the surface and the intermolecular charge transfer. Fig. 6.7(a) depicts the PDOS of TTF and TCNQ of the free independent molecules and the mixed TTF-TCNQ phase.

Upon adsorption, the broadening of the PDOS peaks reflects the hybridization of the molecule with the surface. In the case of TCNQ the width of the orbitals remains unperturbed once the Au(111) surface is introduced in the calculation, meaning a weak surface/molecule interaction. On the other hand, TTF shows an important broadening of the HOMO orbital, from which an important hybridization of the molecule with the surface can be deduced.

The shift of the PDOS expresses the charge transfer between the molecules. TCNQ gains charge (one electron) from the TTF, provoking a shift on both TCNQ HOMO and LUMO towards occupied states. The HOMO becomes totally occupied and the LUMO is pinned at the Fermi level. TCNQ becomes, thus, a magnetic molecule, since its non-degenerated LUMO level is occupied with one electron coming from the TTF. According to the location of the PDOS resonances, DFT confirms that the experimental peaks IS1 and IS2 can not be associated to any specific molecular orbital, since IS1 and IS2 lie in the grey zone marked in Fig. 6.7(a), not crossed by any calculated peak.

The induced charge density calculations corroborate the adsorption and intermolecular charge transfer results from PDOS and add information about the location of the charge. Fig. 6.7 depicts lateral (b) and top (c) views of the distribution of charge. The interaction with the surface (Fig. 6.7(b)) is mainly dominated by the TTF molecule which, similarly as in the individual adsorption case, chemisorbs on the Au(111) surface via two S–Au bonds. The TCNQ/Au(111) interface does not show an important accumulation of charge. Hence, TCNQ is unperturbed by the presence of the substrate, a result that substantiates the PDOS findings. The lateral interaction (Fig. 6.7(c)) demonstrates that TTF and TCNQ still maintain the donor and acceptor character upon adsorption on the metallic surface. TTF loses charge which is accepted by the TCNQ.

The nature of the TTF-TCNQ thin film adsorption and its mixing with the surface can be further explored by resolving the broadened PDOS of the TTF HOMO vs. electron momentum (k) along the symmetry directions of the molecular thin film. Fig. 6.7(d) discloses the existence of two features in the gap between TTF HOMO and LUMO, marked with dashed red (curve) and green (flat) lines. They evidence a more complex structure with TTF character that was hidden behind the broad TTF HOMO resonance calculated at the $\overline{\Gamma}$ point (Fig. 6.7(a)). One of the bands (green) shows a strong TTF character at the $\overline{\Gamma}$ point that vanishes when approaching the $\overline{X}$ point of the surface Brillouin zone (SBZ). The direction $\overline{\Gamma X}$ crosses, in real space, the TTF-TCNQ

molecular rows. Hence, the different weight of TTF orbitals along $\overline{\Gamma X}$ is explained by the heteromolecular nature of the layer along this direction. The other band (red) has a dispersive character and indicates the creation, upon adsorption, of a new metallic-like band that disperses along the molecular rows.

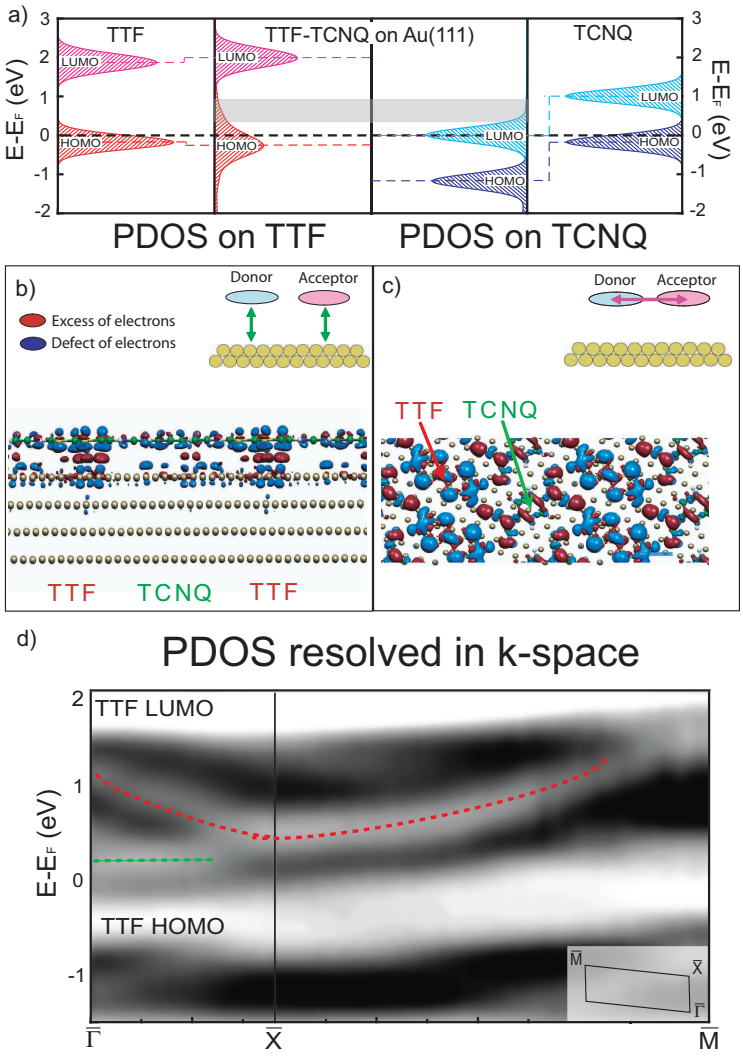

Figure 6.7: (a) From left to right: PDOS of free TTF, TTF mixed on the TTF-TCNQ/Au(111) phase, TCNQ mixed on the TTF-TCNQ/Au(111) phase, and free TCNQ. The grey shadow marks the region energy where the experimental IS1 and IS2 resonances appear.(b) Side and top view of the induce charge density plots on the TTF-TCNQ/Au(111) system (c) PDOS on TTF resolved in k. Red and green dashed lines mark the complex structure arising between HOMO and LUMO of TTF upon TTF-TCNQ adsorption on the Au(111) surface.

Role of metal surface at the TTF-TCNQ/Au(111) interface

To understand the role that the metal surface plays at the metal-organic interface, the calculated band structure is analyzed along the $\overline{\Gamma X}$ and $\overline{XM}$ directions. The three-dimensional location of the charge is examined for every point in the k-space. In Fig. 6.8 the points which show charge located at the organic/metal interface with contribution of the metal surface state are represented. The blue dots correspond to the dispersion of free electrons on the surface state of bare gold. Because of the periodicity introduced in the calculations (TTF-TCNQ unit cell), this band is folded at the $\overline{X}$ point. There are two interface bands dispersing away from $\overline{X}$ which are marked in Fig. 6.8 (a) with the color points red and green. The higher one (red) shows two-dimensional anisotropic dispersion with TTF and metal contributions, while the lower one (green) only exhibits one-dimensional like dispersion along the molecular rows and only presents surface character. Both dispersions have metal-like character with low effective mass values of $0.54m_e$ and $0.44m_e$ for the red and the green band, respectively.

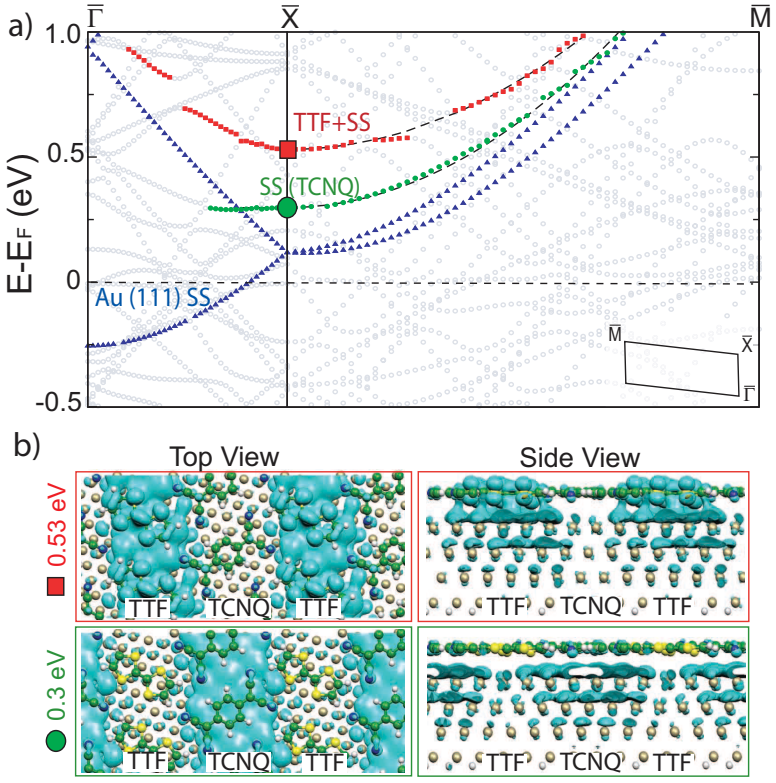

Figure 6.8: (a) Interface band structure along $\overline{\Gamma XM}$ directions. Green and red dots mark states with charge located in the organic-metal interface. Dashed lines along $\overline{XM}$ show the parabolic fit (m* = $0.44m_e$ (green) and $0.54m_e$ (red)). Blue dots mark the pure Au(111) surface state. (b) Constant charge isosurfaces for two states (0.3 eV and 0.53 eV) located at the $\overline{X}$ point of the SBZ. The red band has contributions from both metal and molecular states, while the green band does not exhibit molecular mixing.

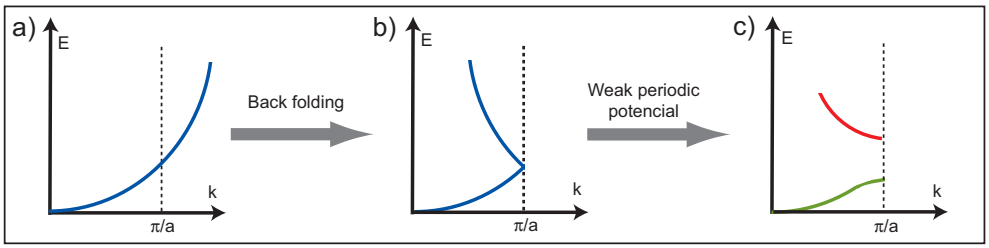

Figure 6.9: Scheme showing the effect of the lattice periodicity (a)-(b) and the anisotropic coupling with the surface (b)-(c).

6.2.2 Periodic potential and formation of hybrid bands

The formation of the two interface bands can be understood from a model of quasi-free electrons in a periodic potential [167] along one surface direction ($\overline{\Gamma X}$). The adsorption of the anisotropic layer on the metal has the following interconnected effects: (i) The periodicity imposed by the TTF-TCNQ layer on the electrons of the surface state folds the surface and bulk bands of the metal inside the first Brillouin zone (1BZ), as reflected in Fig. 6.9(a,b). (ii) The anisotropic coupling with the molecular overlayer (chemisorption of TTF and physisorption of TCNQ) opens a gap at the 1BZ boundary ($\overline{X}$) leading to the upper and lower bands (Fig. 6.9(c)).

The hybrid character of these bands originates from a mixture of folded bulk and surface metal states with TTF states. The charge density at $\overline{X}$ unravels a selective mixing of molecular orbitals with the Au(111) surface state (Fig. 6.8(b)). The red band (at 0.53 eV) corresponds to a strong hybridization of the surface state with the HOMO orbital of the TTF. On the other hand, the green band (at 0.3 eV) has pure surface state character, without molecular mixing.

The symmetry of the molecular adlayer prevents the mixing of the bands, and leads to a spatial separation (Fig. 6.8(b)). The red band is located under the TTF molecular rows, while the pure surface state green band appears below the TCNQ molecules. The fact that we can observe the pure surface state "flowing like a river" below the TCNQ rows is in accord with TCNQ states not interacting with the surface.

Furthermore, the combination of the PDOS resolved in electron momentum-k and the partial charge density plots reveals the variation of the hybrid character of the interface bands along the SBZ (Fig. 6.10). As already stated, the PDOS reflects the density of states corresponding to TTF orbitals, and the plots of charge density are related to the charge located at the organic/metal interface. The red and green guidelines superimposed on the PDOS image act as a guide for the eye, marking the dependence of both PDOS and surface state on electron momentum k. At the $\overline{\Gamma}$ point, the PDOS has strong TTF signal, which vanishes homogeneously for k values approaching the $\overline{X}$ point, at which the state has pure surface state character (lower band at 0.3 eV).

In summary, the comparison between experimental results and DFT calculations allow us to give an answer to the spectroscopy peaks and the dispersive behaviour observed in the conductance maps taken on the molecular layer. The different adsorp-

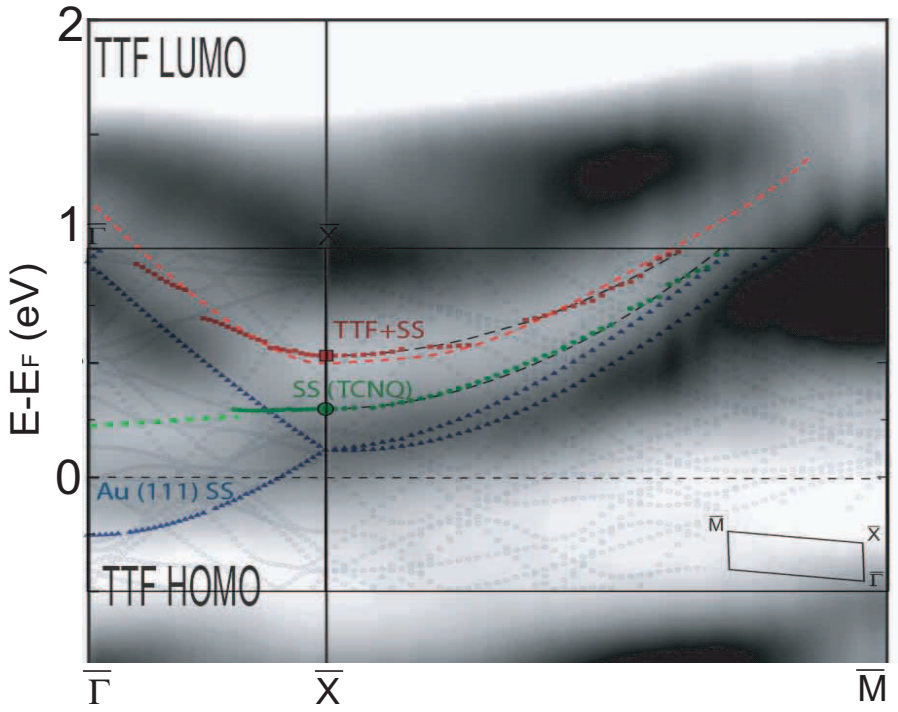

Figure 6.10: Combination of PDOS resolved in k-momentum and the points with density of charge located at the interface. Along direction $\overline{\Gamma X}$ the contribution of the flat band (green dots) develops from mainly molecular (TTF) character at $\overline{\Gamma}$ till pure surface state at $\overline{X}$.

tion properties of TTF and TCNQ on the surface results in the formation of a one-dimensional potential lattice across the molecular rows. As displayed in Fig. 6.11(a), the system draws an analogy to a Kronig-Penney model [168]. The molecular crystal potential along the $\overline{\Gamma X}$ direction would be created by the charge located at the S–Au bonds of the TTF, while the TCNQ would have zero potential since it is considered not to interact with the surface. The solution to the Kronig-Penney model at $\overline{X}$ consists of two wavefunctions, which correspond to our splitted bands (red and green), being the red band located above the TTF rows and the green on the TCNQ rows. As sketched in Fig. 6.11(b), the experimental dI/dV spectra (Fig. 6.3) with IS1 and IS2 resonances localized mainly on TCNQ and TTF rows, respectively, are in agreement with the calculated charge distribution of the organic-metal hybrid bands (red and green branches). Furthermore, the lineshape of the experimental peaks is in accord with the dimensionality of the dispersive bands: IS1 corresponds to a one-dimensional band dispersing along the TCNQ rows, therefore the conductance peak is closer to the shape of a van Hove singularity. IS2 is related to a two-dimensional dispersion, hence it has a broader shape, more related to a step. The quasi-one dimensional dispersive behavior observed along the TCNQ rows (Fig. 6.5) is consistent with the dimensionality and dispersive direction of the calculated green lower band.

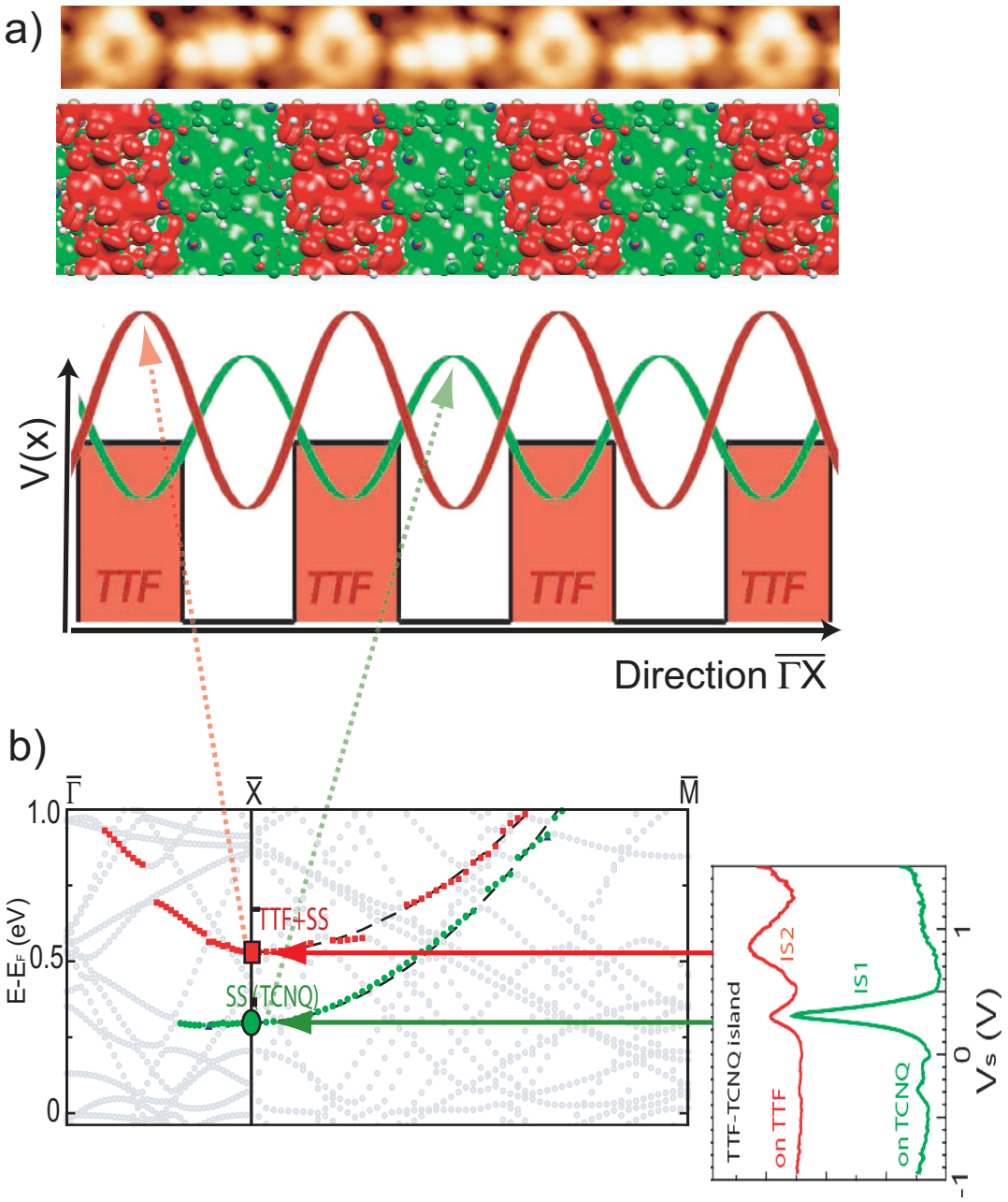

Figure 6.11: (a) Interpretation of the system according to a one-dimensional Kronig-Penney model. The different adsorption strength of TTF and TCNQ generates a potential lattice along $\overline{\Gamma X}$ direction. The two functions which solve this problem would correspond to the hybrid bands with charge located at the surface (b). Comparison between the DFT and the experimental results. The theory explains the spatial location of resonances IS1 and IS2 and the dispersive behavior observed on the TCNQ rows.

6.3 Conclusions

In this section we have characterized the co-adsorption of TTF and TCNQ on Au(111), both structurally and electronically. TTF and TCNQ mix spontaneously in a highly anisotropic molecular layer when deposited at room temperature. The molecules are organized in homomolecular rows of TTF and TCNQ, similar to the bulk distribution, with the difference that molecules lay planar to the surface. As a result, the self-assembled phase is stabilized via hydrogen bonds. Even with this planar configuration, the donor-acceptor character of both molecules survives on the presence of the metallic surface as proven by DFT calculations.

The interaction of such anisotropic adlayer with a metallic surface results in a selective mixing of surface and molecular states. The different adsorption strength of TTF and TCNQ generates a potential across the molecular rows and creates two hybrid metal-like dispersive bands, spatially separated on the molecular stacks. One of them, located on the TCNQ rows, has pure surface state character and disperses one-dimensionally like along the molecular rows, explaining the dispersion observed experimentally on the TCNQ chains. The second one, located on the TTF rows, presents a mixture of surface state and molecular orbital (HOMO). In this case the band disperses two-dimensionally but such dispersion has not been detected by dI/dV maps due to its strong mixing with molecular orbitals.